

Light-emitting defects and epitaxy in alkali-ion-implanted α quartz

J. Keinonen, S. Gašiorek, P. K. Sahoo, S. Dhar, and K. P. Lieb

Citation: [Applied Physics Letters](#) **88**, 261102 (2006); doi: 10.1063/1.2215615

View online: <http://dx.doi.org/10.1063/1.2215615>

View Table of Contents: <http://scitation.aip.org/content/aip/journal/apl/88/26?ver=pdfcov>

Published by the [AIP Publishing](#)

Articles you may be interested in

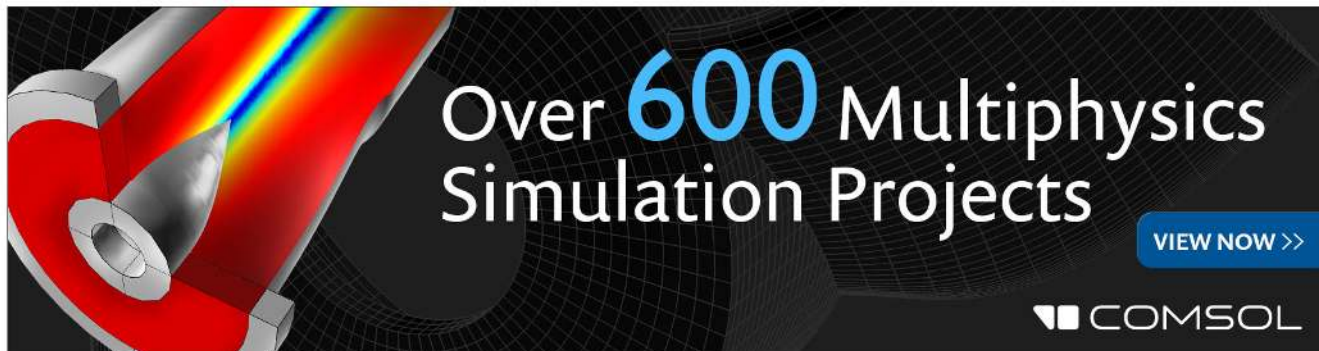
[Solid-phase epitaxy of silicon amorphized by implantation of the alkali elements rubidium and cesium](#)
AIP Conf. Proc. **1496**, 276 (2012); 10.1063/1.4766542

[Effect of stress on the evolution of mask-edge defects in ion-implanted silicon](#)
J. Vac. Sci. Technol. B **24**, 446 (2006); 10.1116/1.2162566

[Achieving epitaxy and intense luminescence in Ge/Rb-implanted \$\alpha\$ -quartz](#)
Appl. Phys. Lett. **87**, 021105 (2005); 10.1063/1.1994953

[Cathodoluminescence versus dynamical epitaxy of Ba-ion irradiated \$\alpha\$ -quartz](#)
Appl. Phys. Lett. **85**, 1341 (2004); 10.1063/1.1784538

[Chemically guided epitaxy of Rb-irradiated \$\alpha\$ -quartz](#)
J. Appl. Phys. **95**, 4705 (2004); 10.1063/1.1689733

The advertisement features a 3D cutaway of a mechanical part with a rainbow-colored stress or temperature distribution. The text 'Over 600 Multiphysics Simulation Projects' is prominently displayed in white and blue. A blue button with white text says 'VIEW NOW >>'. The COMSOL logo is in the bottom right corner.

Over **600** Multiphysics
Simulation Projects

[VIEW NOW >>](#)

COMSOL

Light-emitting defects and epitaxy in alkali-ion-implanted α quartz

J. Keinonen,^{a)} S. Gašiorek,^{b)} P. K. Sahoo,^{c)} S. Dhar,^{d)} and K. P. Lieb^{e)}

II. Physikalisches Institut, Universität Göttingen, Friedrich-Hund-Platz 1, D-37077 Göttingen, Germany

(Received 8 December 2005; accepted 22 May 2006; published online 27 June 2006)

Light-emitting centers in alkali-ion-implanted α quartz have been investigated with respect to the solid phase epitaxial growth of the ion irradiation induced amorphous zone. Cathodoluminescence was studied under the conditions of chemical epitaxy in annealing the samples, implanted with 2.5×10^{16} 50 keV Na ions/cm² or 175 keV Rb ions/cm², in ¹⁸O₂ atmosphere in the temperature range of 673–1173 K. In addition to the known intrinsic subbands at 2.40, 2.79, and 4.30 eV, which previously were associated with specific defects in the silica matrix, a strong violet band at 3.65 eV and a band at 3.25 eV have been identified. Both are intimately correlated with the presence of the implanted alkali atoms and recrystallization process. With respect to the 3.25 eV band reported in the literature, they are discussed to be correlated with the presence of nanoclusters in Si-enriched, and Ge- and Sn-implanted SiO₂ structures. © 2006 American Institute of Physics.

[DOI: 10.1063/1.2215615]

The amorphous and crystalline forms of silicon dioxide doped with group-IV or rare earth atoms and nanoclusters are important materials for optoelectronics, photonic, and microelectronic device fabrication.^{1–4} Defect production and annihilation by energetic ion bombardment and thermal annealing are essential technological issues for understanding the defect dynamics responsible for the optical properties of SiO₂. Doping α quartz with ions substituting Si in the crystalline SiO₂ matrix may be a challenging step to tailor novel optical properties suitable for quantum semiconductor devices.⁵ As quartz amorphizes easily under the impact of low fluences of heavy ions,⁶ attempts of dynamic, chemical, or laser-induced solid phase epitaxial growth of such amorphized layers have been made in order to remove radiation damage induced during implantation.^{7–20}

In this work, we report on a defect center obtained in alkali-ion-implanted α quartz. It is related to the implanted alkali ions Na and Rb and recrystallization of the matrix. We discuss the cathodoluminescence (CL) spectra obtained during the epitaxy. We identify CL emission bands associated with the implanted ions and the recrystallization process and distinguish them from the intrinsic bands, which are related to defect structures of the matrix due to any ion or electron bombardment or any other defect production mechanism.

Our experimental approach is different from that used in previous works, where luminescence related to the structures of the interface between Si, Ge, and Sn nanoclusters and SiO₂ matrix was studied, e.g., Refs. 21–23. We implanted α quartz with alkali ions followed by annealing in oxygen atmosphere, a process called chemical epitaxy, because it produces full planar recrystallization of the amorphous region under specific processing conditions.^{9–12} This was expected

to provide information on the microscopic structure of defect centers in strongly damaged SiO₂.

Single-crystalline α -quartz (0001) substrates, $10 \times 10 \times 1$ mm³ in size, were homogeneously implanted at liquid nitrogen temperature to a fluence of 2.5×10^{16} ions/cm² with 50 keV Na⁺ ions and 175 keV Rb⁺ ions from the Göttingen implanter IONAS. The beam current was 1.5 μ A. To obtain chemical epitaxy, the amorphized samples were annealed for 1 h in ¹⁸O₂ atmosphere (98% enriched in ¹⁸O) between 673 and 1173 K. Each sample was enclosed inside a quartz ampoule. The recrystallization of the radiation-damaged profile in the matrix, which is connected to the lattice locations of the atoms, was observed by means of Rutherford backscattering spectrometry and channeling (RBS-C) measurements using a 15 nA beam of 0.9 MeV α particles from IONAS. Depth profiles of the implanted Na and Rb atoms, Si, ¹⁶O, and ¹⁸O, and ¹²C, ¹H and other possible impurities were obtained in time-of-flight elastic-recoil-detection (TOF-ERD) analysis at the 5 MV tandem accelerator of the University of Helsinki.^{24,25} For details of the RBS-C and ERD analysis, see Ref. 11 and references therein.

The dependence of the volume fraction (f_v) of the amorphized zone (initially about 200 nm in Na implantations and 280 nm in Rb implantations) on the annealing temperature is shown in Fig. 1(a). In the Rb-implanted samples the crystallization front started to move towards the surface at about 950 K. At $T_X=1060$ K, half the amorphous volume had recrystallized and full solid phase epitaxial growth (SPEG) was completed at 1123 K. Also when annealing the Na-implanted samples, a planar recovery of the damaged region was observed at a typical temperature of $T_X \approx 930$ K.

Figure 1(b) illustrates the outdiffusion of the implanted Rb atoms. Heating of the samples led to rapid migration of the implanted Rb to the surface, where it evaporated. At 1000 K any possible concentration left was below the RBS detection limit of 0.1 at. %. We define the outdiffusion temperature T_D , at which half the implanted ions have left the samples: $T_D(\text{Rb})=860$ K. Also when annealing the Na-implanted samples, the back edge of the implanted Rb profile located at the amorphous/crystalline (a/c) interface was pushed out of the recovering zone, giving $T_D(\text{Na}) \approx 930$ K. For both Na- and Rb-implanted samples, a large amount of

^{a)}Permanent address: Accelerator Laboratory, University of Helsinki, FI-00014 Helsinki, Finland.

^{b)}Present address: Laser-Laboratorium Göttingen e.V., D-37077 Göttingen, Germany.

^{c)}Present address: Instituut voor Kern-en Stralingsfysica, K. U. Leuven, B-3001 Leuven, Belgium.

^{d)}Present address: Physics Department, University of Maryland, College Park, MD.

^{e)}Author to whom correspondence should be addressed; electronic mail: plieb@gwdg.de

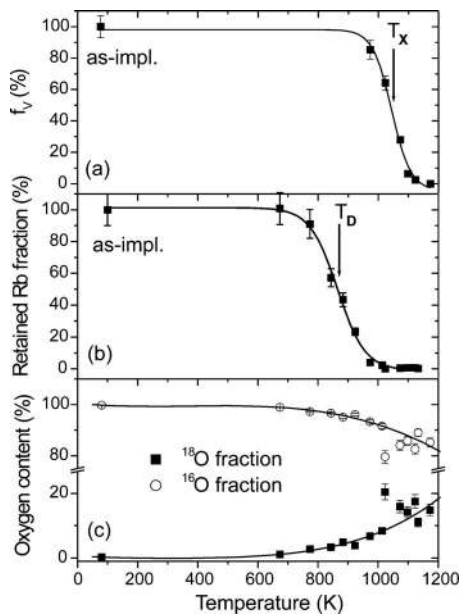


FIG. 1. Temperature dependence of (a) the volume fraction f_v of amorphous SiO_2 in the implanted region, (b) the retained fraction of implanted Rb ions, and (c) the increase in the ^{18}O atomic fraction and decrease in the ^{16}O atomic fraction in the implanted region.

the external ^{18}O annealing gas was found to diffuse inside the SiO_2 matrix and a corresponding amount of ^{16}O to diffuse out of the matrix. However, no change in the total oxygen concentration was observed.^{11,12} The temperature dependence of this exchange process after Rb implantation is illustrated in Fig. 1(c).

The CL measurements were performed using a 5 keV electron beam, whose current (power density) was maintained at $2 \mu\text{A}$ (1 W/cm^2). The sample temperature was kept at room temperature (RT). The luminescence light was detected by a Hamamatsu R928 photomultiplier after focusing it into a Czerny-Turner spectrograph (Jobin Yvon 1000M). CL spectra were collected in the wavelength range from 200 to 900 nm at a speed of 1 nm/s with a 1200 lines/mm grating. The 300 nm range of the CL analysis covers the amorphous zones produced in the implantations.

The measured CL spectra are illustrated in Figs. 2(a)–2(c). Figure 2(a) shows the intrinsic peaks taken for samples of pure α quartz, fused silica, α - SiO_2 on Si, and α quartz amorphized by the irradiation of 800 keV Ba ions. Note that the range of the Ba ions is far beyond the range of the CL analysis. Figures 2(b) and 2(c) illustrate the CL spectra measured after Rb and Na implantations, respectively, and annealing in $^{18}\text{O}_2$ gas. The shapes and intensities of these spectra exhibit rather dramatic changes as a function of the annealing temperature. The CL spectra, including several broad and narrow peaks, were deconvoluted with Gaussian-shaped subbands. The CL emission intensities of all the subbands were corrected for the instrument response function, which was determined by using a standard halogen calibration lamp. In the fits we adopted the CL fingerprints of the known intrinsic subbands at 2.40, 2.79, and 4.30 eV, which are shown in Fig. 2(a) and were introduced in Refs. 26–29.

In addition, we obtained violet bands at 3.25 and 3.65 eV. They belong to the second category of luminescence centers, where defects are correlated with particular species in the SiO_2 matrix introduced by ion implantation. A strong 3.25 eV band was previously identified in connection

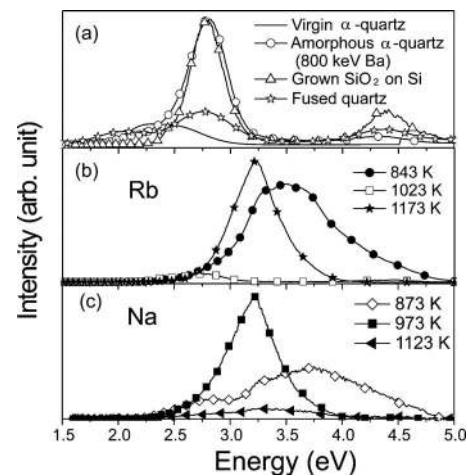


FIG. 2. (a) CL spectra showing the intrinsic bands for samples of pure α quartz, fused silica, α - SiO_2 on Si, and α quartz amorphized by the implantation of 800 keV Ba ions. (b) CL spectra of Rb-implanted samples taken after annealing at different temperatures. (c) As (b) but for Na-implanted samples.

with Si, Ge, and Sn nanoclusters in SiO_2 (Refs. 14, 17, and 21–23). Up to now, the 3.65 eV band has not been reported in the literature. The temperature dependence of the 3.25 and 3.65 eV band intensities is shown in Figs. 3(b) and 3(c) for the Rb and Na-implanted samples, respectively. The characteristic temperatures for alkali-ion outdiffusion (T_D) and full epitaxy of the matrix (T_x) are indicated. The fact that the decrease in the intensity of the 3.65 eV band strongly correlates with the fraction of alkali ions retained in the matrix is of utmost importance. The rise in the 3.25 eV intensity correlates with the increase in the crystalline volume fraction ($1-f_v$) of the implanted region.

As discussed by Stevens-Kalceff and collaborators^{26–28} particular defect configurations and luminescence mechanisms were proposed for the intrinsic bands.^{26–31} The facts that we have only observed a 2.40 eV line in the case of virgin α quartz [Fig. 2(a)] and that it is present with a constant intensity in all the annealed samples indicate that this band is connected to the electron-beam-induced vacancy interstitial pairs ($V_{\text{O}}; \text{O}_2$) (Ref. 30) in the CL electron bombardment. The 2.79 and 4.30 eV bands observed in the cases of Ba-irradiation-amorphized quartz, SiO_2 grown on Si, and fused quartz are related to ODC-type defects.^{27,28} They are

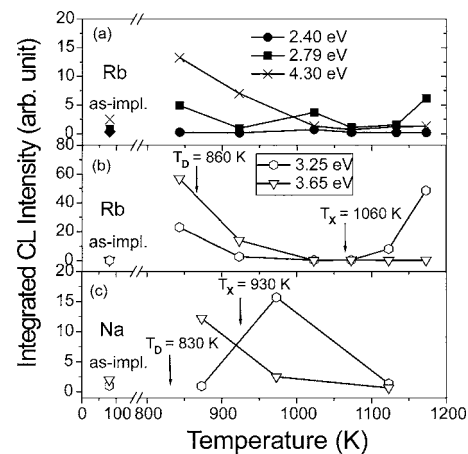
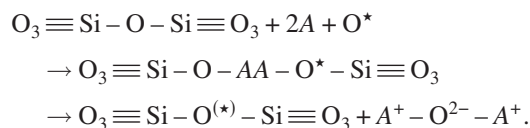


FIG. 3. Temperature dependence of the intensities of the intrinsic 2.40, 2.79, and 4.30 eV bands as obtained in the Rb-implanted samples (a), of the 3.25 and 3.65 eV bands in Rb-implanted samples (b), and in Na-implanted samples (c).

present in all strongly damaged SiO₂ structures and did not anneal out in the temperature region used.

We assume the 3.65 eV band to be due to the defect center O₃≡Si–O–A, i.e., an atomic configuration, where the alkali ion (A) is connected to a dangling oxygen bond of the nonbridging oxygen-hole center (O≡Si–O[•]). This configuration is produced during the epitaxial regrowth, where the effect of implanted alkali ions and migrating oxygen (O^{*}) is described as^{9,11}



O^{*} denotes external ¹⁸O and O^(*) refers to either ¹⁸O or ¹⁶O. Note that as the A–O bond is energetically weaker (≈3 eV) than the Si–O bond (4.57 eV), annealing disrupts first the alkali-oxygen bond leading to alkali diffusion and then the silicon-oxygen bond, which leads to E' center (O≡Si[•]). There are several hints, which support this interpretation:

- The 3.65 eV band has only been observed after alkali ion implantation, but neither after Ge nor Ba ion implantation.^{13,14}
- The 3.65 eV band disappears to the extent the alkali ions diffuse out of the samples, as Figs. 3(b) and 3(c) indicate for Rb and Na. This has also been found after Cs-ion implantation and partial epitaxy induced by excimer-laser annealing.¹⁹

The intense photoluminescence (PL) at 3.25 eV from nanoparticles in gas-suspended SiO_x,²¹ and Ge- and Sn-implanted SiO₂ layers,^{22,23} has been attributed to the formation of neutral oxygen vacancies (NOVs) in ≡Si–Si≡, ≡Ge–Ge≡, ≡Ge–Si≡, ≡Sn–Sn≡, and ≡Si–Sn≡ structures. These moleculelike luminescence centers have a three-level energy system, in which blue-violet emission (≈3.2 eV) and UV emission (≈4.25 eV) are due to triplet-to-singlet (T₁→S₀) and singlet-to-singlet (S₁→S₀) transitions, respectively. In the current experiment, the 3.25 eV line also appears connected to the formation of the NOV structure ≡Si–Si≡. During chemical epitaxy, the matrix network is modified in such a way that E' centers (O≡Si[•]) are produced and join to form the NOV structure.

Annealing the Na-implanted samples at temperatures clearly above T_X led to the dissociation of the NOVs. Such temperatures were not reached for the Rb-implanted samples. In Ge-implanted α-quartz samples, a saturated increase in the 3.25 eV CL intensity has been observed when only about 40% of the full SPEG was achieved and the content of implanted Ge atoms stayed constant.¹⁴ In double implanted Rb/Ge samples, no loss of Ge atoms but a complete loss of Rb atoms and full SPEG led to a high CL intensity of the 3.25 eV line.¹⁷ The PL emission from single-crystal Ge and Sn nanoparticles, revealed by high-resolution transmission electron microscopy, was related to NOVs around the nanoparticles.^{22,23} We conclude that the formation of the NOV structures between group-IV atoms indicated by the intensive 3.25 eV light relates to a strongly damaged SiO₂ matrix.

In conclusion, we have identified a photoactive defect structure indicated by the intense 3.65 eV violet band in the

CL spectra in the chemical epitaxy of alkali-ion-implanted (Na, Rb) α quartz. We also tentatively explain how the formation of NOV structures in these samples, corresponding to the 3.25 eV band, is connected to the recrystallization of the implanted region in chemical annealing. Finally, we have observed that the 2.4 eV CL band is due to electron-irradiation-induced defects in quartz.

Deutsche Forschungsgemeinschaft (DFG), Deutscher Akademischer Austauschdienst (DAAD), and the Academy of Finland supported this work. The authors would like to thank Professor Hans Hofsäb, Detlev Purschke, and Dr. Michael Uhrmacher for their help and support.

- H. Hosono, *J. Non-Cryst. Solids* **187**, 457 (1995).
- L. Rebohle, J. Von Borany, W. Skorupa, H. Förb, and S. Niedermeier, *Appl. Phys. Lett.* **77**, 969 (2000).
- Y. Q. Wang, G. L. Kong, W. D. Chen, H. W. Diao, C. Y. Chen, S. B. Zhang, and X. B. Liao, *Appl. Phys. Lett.* **81**, 4174 (2002).
- A. V. Kabashin and M. Meunier, *Appl. Phys. Lett.* **82**, 1619 (2003).
- Y. C. Fang, W. Q. Li, L. J. Qi, L. Y. Li, Y. Y. Zhao, Z. J. Zhang, and M. Lu, *Nanotechnology* **15**, 494 (2004).
- F. Harbsmeier and W. Bolse, *J. Appl. Phys.* **83**, 4049 (1998).
- G. Devaud, C. Hayzelden, M. J. Aziz, and D. Turnbull, *J. Non-Cryst. Solids* **134**, 129 (1991).
- S. Dhar, W. Bolse, and K. P. Lieb, *J. Appl. Phys.* **85**, 3120 (1999).
- F. Roccaforte, W. Bolse, and K. P. Lieb, *Appl. Phys. Lett.* **73**, 134 (1998); *J. Appl. Phys.* **89**, 3611 (2001); F. Roccaforte, F. Harbsmeier, S. Dhar, and K. P. Lieb, *Appl. Phys. Lett.* **76**, 3709 (2000).
- M. Gustafsson, F. Roccaforte, J. Keinonen, W. Bolse, L. Ziegeler, and K. P. Lieb, *Phys. Rev. B* **61**, 3327 (2000).
- S. Gąsiorek, S. Dhar, K. P. Lieb, T. Sajavaara, and J. Keinonen, *J. Appl. Phys.* **95**, 4705 (2004).
- S. Dhar, S. Gąsiorek, M. Lang, K. P. Lieb, J. Keinonen, and T. Sajavaara, *Surf. Coat. Technol.* **158/159**, 436 (2002).
- S. Dhar, S. Gąsiorek, P. K. Sahoo, U. Vetter, H. Hofsäb, V. N. Kulkarni, and K. P. Lieb, *Appl. Phys. Lett.* **85**, 1341 (2004); *J. Appl. Phys.* **97**, 014910 (2005).
- P. K. Sahoo, S. Dhar, S. Gąsiorek, and K. P. Lieb, *Nucl. Instrum. Methods Phys. Res. B* **216**, 324 (2004); *J. Appl. Phys.* **96**, 1392 (2004).
- S. Gąsiorek, P. K. Sahoo, S. Dhar, K. P. Lieb, K. Arstila, and J. Keinonen, *Appl. Phys. B: Lasers Opt.* (online).
- S. Gąsiorek, P. K. Sahoo, S. Dhar, K. P. Lieb, T. Sajavaara, and J. Keinonen, *J. Non-Cryst. Solids* (in press).
- P. K. Sahoo, S. Gąsiorek, K. P. Lieb, K. Arstila, and J. Keinonen, *Appl. Phys. Lett.* **87**, 021105 (2005).
- S. Gąsiorek, P. K. Sahoo, K. P. Lieb, and P. Schaaf, *Appl. Surf. Sci.* **247**, 396 (2005).
- P. K. Sahoo, S. Gąsiorek, S. Dhar, K. P. Lieb, and P. Schaaf, *Appl. Surf. Sci.* **252**, 4477 (2006).
- K. P. Lieb, in *Encyclopedia on Nanoscience and Nanotechnology*, edited by H. S. Nalwa (American Scientific, Stevenson Ranch, CA, 2004), Vol. 3, pp. 233–251.
- D. B. Geohegan, A. A. Puretzi, G. Duscher, and S. J. Pennycook, *Appl. Phys. Lett.* **73**, 438 (1998).
- J. M. J. Lopes, F. C. Zawislak, M. Behar, L. Rebohle, and W. Skorupa, *J. Appl. Phys.* **94**, 6059 (2003).
- J. M. J. Lopes, F. C. Zawislak, P. F. P. Fichtner, F. C. Lovey, and A. M. Condó, *Appl. Phys. Lett.* **86**, 023101 (2005).
- J. Jokinen, J. Keinonen, P. Tikkanen, A. Kuronen, T. Ahlgren, and K. Nordlund, *Nucl. Instrum. Methods Phys. Res. B* **119**, 533 (1996).
- K. Arstila, T. Sajavaara, and J. Keinonen, *Nucl. Instrum. Methods Phys. Res. B* **174**, 163 (2001).
- M. A. Stevens-Kalceff and M. R. Philips, *Phys. Rev. B* **52**, 3122 (1995).
- M. A. Stevens-Kalceff, *Phys. Rev. B* **57**, 5674 (1998); *Phys. Rev. Lett.* **88**, 3137 (2000).
- M. A. Stevens-Kalceff and J. Wong, *J. Appl. Phys.* **97**, 113519 (2005).
- L. Skuja, B. Gütler, D. Schiel, and A. R. Silin, *Phys. Rev. B* **58**, 14296 (1998).
- H.-J. Fitting, T. Barfels, A. N. Trukhin, and B. Schmidt, *J. Non-Cryst. Solids* **279**, 51 (2001).
- M. Yoshikawa, K. Matsuda, Y. Yamaguchi, T. Matsunobe, Y. Nagasawa, H. Fujino, and T. Yamane, *J. Appl. Phys.* **92**, 7153 (2002).